

Tailoring steep density profile with unstable points

Shun Ogawa*

*Laboratory for Neural Computation and Adaptation,
RIKEN Center for Brain Science,
2-1 Hirosawa Wako Saitama 351-0198, Japan*

Xavier Leoncini

Aix Marseille Univ, Université de Toulon, CNRS, CPT, Marseille, France[†]

Alexei Vasiliev

Space Research Institute, Profsoyuznaya 84/32, Moscow 117997, Russia

Xavier Garbet

CEA, IRFM, F-13108 St. Paul-lez-Durance cedex, France

The mesoscopic properties of a plasma in a cylindrical magnetic field are investigated from the view point of test-particle dynamics. When the system has enough time and spatial symmetries, a Hamiltonian of a test particle is completely integrable and can be reduced to a single degree of freedom Hamiltonian for each initial state. The reduced Hamiltonian sometimes has unstable fixed points (saddle points) and associated separatrices. To choose among available dynamically compatible equilibrium states of the one particle density function of these systems we use a maximum entropy principle and discuss how the unstable fixed points affect the density profile or a local pressure gradient, and are able to create a steep profile that improves plasma confinement.

Being able to sustain a steep density profile in hot magnetized plasma is one of the major key points to achieve magnetically confined fusion devices. These steep profiles are typically associated with the emergence in the plasma of so-called internal transport barriers (ITB) [1, 2]. Both the creation and study of these barriers have generated numerous investigations mostly numerical using either a fluid, or magnetic field or kinetic perspective or combining some of these. In this paper starting from the direct study of particle motion, we propose a simple mechanism to set up a steep profile which may not have been fully considered yet. Indeed, charged particle motion in a non-uniform magnetic field [3–9] is one of main classical issues of physics of plasmas in space or in fusion reactors. To tackle this problem the guiding center [7] and the gyrokinetic [8] theories are developed to trace the particle’s slower motion by averaging the faster cyclotron motion. These reductions suppress computational cost and they are widely used to simulate the magnetically confined plasmas in fusion reactors [6]. These reduction theories assume existence of an invariant or an adiabatic invariant of motion associated with the magnetic moment. Meanwhile, this assumption does not always hold true. Then, recently, studies on full particle orbits without any reductions are done to look into phenomena ignored by these reductions and to interpolate the guiding center orbit. There exists a case that a guiding center trajectory and a full trajectory are completely different [10]. Further, it is found that the assumption of the invariant magnetic moment breaks [11, 12] due to the chaotic motion of the test particles.

Let us quickly review the single particle motion and adiabatic chaos. We consider a model of charged particle moving in a non-uniform cylindrical magnetic field $\mathbf{B}(r) = \nabla \wedge \mathbf{A}_0(r)$. The vector potential $A_0(r)$ is given by

$$\mathbf{A}_0(r) = \frac{B_0 r}{2} \mathbf{e}_\theta - B_0 F(r) \mathbf{e}_z, \quad F(r) = \int_0^r \frac{r dr}{R_{\text{per}} q(r)}, \quad (1)$$

where the cylinder is parametrized with the coordinate (r, θ, z) , B_0 is strength of the magnetic field, z has $2\pi R_{\text{per}}$ -periodicity, \mathbf{e}_θ and \mathbf{e}_z are basic units for each direction, and $q(r)$ is a winding number called a safety factor of magnetic field lines. The Hamiltonian of the particle $H = \|\mathbf{v}\|^2/2$, where \mathbf{v} denotes particle’s velocity, has three constants of motion, the energy, the angular momentum, and the momentum, associated with time, rotational, and translational symmetry of the system respectively, so that the Hamiltonian H on the six dimensional phase space is reduced into the single-degree-of-freedom Hamiltonian on the two dimensional phase space, (r, p_r) -plane [11, 12],

$$H_{\text{eff}}(r, p_r) = p_r^2/2 + V_{\text{eff}}(r), \\ V_{\text{eff}}(r) = \frac{v_\theta^2 + v_z^2}{2} = \frac{(p_\theta r^{-1} - B_0 r/2)^2}{2} + \frac{(p_z + B_0 F(r))^2}{2}. \quad (2)$$

where p_i stands for the conjugate momentum for $i = r, z$, and θ respectively, and where $v_\theta = r\dot{\theta}$ and $v_z = \dot{z}$. The upper dot denotes d/dt . Invariants p_z and p_θ are fixed by the initial condition of the particle in the 6-dimensional phase space. Appropriately setting the safety factor q and choosing initial condition, we can find an unstable fixed point in (r, p_r) phase plane, which can induce the adiabatic chaos [13–17] when the weak magnetic perturbation or the curvature effect added to the flat torus (cylinder) exist [11, 12].

* shun.ogawa@riken.jp

[†] Xavier.Leoncini@cpt.univ-mrs.fr

This Letter aims to exhibit one possibility that the unstable fixed point inducing chaotic motion modifies mesoscopic properties of plasmas, local density and pressure gradients which are believed to be associated with the internal transport barriers (ITBs) [1, 2] a feature missed by gyrokinetics, or a pure magneto-hydrodynamic approach. For this purpose, we shall compute an equilibrium radial density function $\rho(r)$ from stationary kinetic distribution. When neglecting the feedback on the fields of the motion of the particles governed by the Hamiltonian (2) computing a stationary state of an ensemble of particles, i.e. a stationary one-particle density function, resumes to find a density function f_0 on the phase space, which commutes with Hamiltonian (2). Since the motion is integrable, these solutions correspond after a local change to action-angle variables to functions depending only on the actions of the Hamiltonian with a uniform distribution of the associated angles (see for instance for a similar situation [23]). As a consequence, there exist infinitely many steady states. In order to choose one, we may assume a vanishing collisionality, and consider that the one maximizing the information entropy under suitable constraint conditions is picked out [22, 24]. In principle, we should consider a Vlasov-Maxwell system consisting of the collisionless Boltzmann equation describing a temporal evolution of single particle density functions of ions and electrons, coupled with the Maxwell equation determining a self-consistent electro-magnetic field [20, 21], when neglecting the self-consistency we notably neglect electrons (their presence insures a neutralizing background, and the current to get the right poloidal component of magnetic field), inter-particle interactions, radiation from moving charged particles and back reaction from the electro-magnetic field. As such we are looking for a steady state of a truncated Vlasov-Maxwell system with an ion moving in a static magnetic field. In this setting we qualitatively discuss which kind of vector potentials $F(r)$ or q -profiles are likely to bring about the unstable fixed point for the test particle motion. Then, we look into the effect of the unstable fixed point for the density profile and the local-pressure gradient. We shall end this Letter by remarking the relation between the steep density profile (particle's ITBs) and the magnetic ITBs [18, 19].

Among the different stationary distributions, let us now compute the general form of f_0 which maximizes the information entropy (also called a density of the Boltzmann Gibbs. The Boltzmann's constant k_B is set as unity. We thus have to maximize the functional

$$\mathcal{S}[f] = - \iint_{\mu} f \ln f d^3 \mathbf{p} d^3 \mathbf{q}, \quad (3)$$

subject to the normalization condition (conservation of the number of particles) and energy, momentum, and angular momentum conservations, which are respectively

$$\begin{aligned} \mathcal{N}[f] &= \iint_{\mu} f d^3 \mathbf{p} d^3 \mathbf{q}, \quad \mathcal{E}[f] = \iint_{\mu} H_{\text{eff}} f d^3 \mathbf{p} d^3 \mathbf{q}, \\ \mathcal{P}[f] &= \iint_{\mu} p_z f d^3 \mathbf{p} d^3 \mathbf{q}, \quad \mathcal{L}[f] = \iint_{\mu} p_{\theta} f d^3 \mathbf{p} d^3 \mathbf{q}, \end{aligned} \quad (4)$$

where the integral $\iint_{\mu} \bullet d^3 \mathbf{p} d^3 \mathbf{q}$ means average over the six dimensional single particle phase space, noted here μ -space. The solution to this variational problem is

$$f_0 = e^{-\beta H_{\text{eff}} - \gamma_1 p_{\theta} - \gamma_z p_z} \quad (5)$$

where β , γ_1 , γ_{θ} , and γ_z are the Lagrangian multipliers, associated with energy conservation, normalization, momentum and angular momentum conditions respectively. The parameter β corresponds to the thermodynamical temperature as

$$T_{\text{th}}^{-1} \equiv \beta = \delta \mathcal{S} / \delta \mathcal{E}, \quad (6)$$

and it can be safely assumed positive. It should be noted that $-\gamma_{\theta}$ and $-\gamma_z$ are proportional to the ensemble averages of v_{θ} and v_z respectively. In the literature is has been admitted that when an ITB exists plasma rotation exists. We then expect that in such state the averages of v_{θ} and v_z are not 0 and so are γ_{θ} and γ_z . The spatial density function $n(q)$ is deduced from this result as

$$n(\mathbf{q}) \equiv \int f_0 d^3 \mathbf{p} = \int f_0 r^{-1} dp_{\theta} dp_z dp_r. \quad (7)$$

Thus, the density $n(r)d^3 q$ is proportional to

$$n(\mathbf{q}) r dr d\theta dz \propto e^{\left(\frac{\gamma_{\theta}}{2} \left(-B_0 - \frac{\gamma_{\theta}}{\beta}\right) r^2 + \gamma_z B_0 F(r)\right)} r dr d\theta dz, \quad (8)$$

and is independent of θ and z . We then obtain a radial density function $\rho(r)$ given by

$$\rho(r) = \frac{\iint n(\mathbf{q}) r dr d\theta dz}{\iint r dr d\theta dz} = \frac{1}{4\pi^2 r R_{\text{per}}} \iint n(\mathbf{q}) r dr d\theta dz, \quad (9)$$

as

$$\begin{aligned} \rho(r) &= \frac{\exp(-ar^2 - bF(r))}{\int_0^{\infty} \exp(-ar^2 - bF(r)) dr}, \\ a &= \frac{\gamma_{\theta}}{2} \left(B_0 - \frac{\gamma_{\theta}}{\beta} \right), \quad b = -\gamma_z B_0. \end{aligned} \quad (10)$$

We can notice from Eq.(10) that the equilibrium profile is not flat as soon as γ_{θ} is not zero and that it depends on the poloidal magnetic field configuration when $\gamma_z \neq 0$. Given the definitions, this means as soon as the plasma moves the profiles are not flat. Since we are considering an equilibrium configuration, we may as well end up with a non-flat temperature profile, but here we have to consider the local radial kinetic temperature of the particles rather than the thermodynamic one (6), so this would correspond to the average of the energy at constant radius. In the same spirit as for the density we can compute the spatial energy density function $\varepsilon(q)$ is deduced from this result as

$$\varepsilon(\mathbf{q}) \equiv \int f_0 H_{\text{eff}} d^3 \mathbf{p} = \int f_0 H_{\text{eff}} r^{-1} dp_{\theta} dp_z dp_r. \quad (11)$$

Thus, we notice that

$$\varepsilon(\mathbf{q}) = -\frac{\partial n(\mathbf{q})}{\partial \beta} \quad (12)$$

so the kinetic temperature profile $T(r)$ is proportional to $\rho(r)$. In the same spirit it should be noted that the local pressure $P(r)$ is proportional to the radial density $\rho(r)$, because we assume the equation of state $P(r) = N\rho(r)T_{\text{th}}$ holds locally true, where N is the number of particles and here we consider the equilibrium temperature T_{th} .

We now move on and consider how the existence of the unstable fixed points with relevant energy level affects the obtained equilibrium density profile. For this purpose we have to discuss how the safety factor is chosen, in other words which function F in Eq. (1) leads to the emergence of “practical” unstable points in the effective potential V_{eff} . Indeed, as a first point to pin out, if the amplitude of F is large, we can expect that the term $v_z^2/2 = (p_z + F)^2/2$ in the Hamiltonian (2) becomes also large, then the unstable points appear in the phase space at so high energy level that they become physically irrelevant. Therefore, the amplitude of F should be small.

Moreover if the variations of $F(r)$ are smooth and “gentle” with r , so does again $(p_z + F)^2/2$ in V_{eff} , then V_{eff} has only one minimum point that is essentially governed by the term $(p_\theta/r - B_0 r/2)^2/2$. Thus, enough concavity of $v_z^2/2$ near but not at the minimum point of $(p_\theta/r - B_0 r/2)^2/2$, $r = \sqrt{2p_\theta/B_0}$ is necessary so that V_{eff} has unstable points. These considerations are illustrated in Fig. 1. In the panel (d), we assume that there exists an r such that $p_z + F(r) = 0$. We stress out as well that if $|p_z|$ is sufficiently large, it is also possible to create an unstable point, but then again the energy level is so high that it is irrelevant for the mesoscopic profiles in considered plasmas.

Given the obtained density profile (10), we can notice that a sudden fast variation of the function F , will lead to strong variations of the profile, as long as r is not too large, for instance a step like profile should translate in a steep profile. With this in mind, since this effect is present if γ_z , related to the average velocity along the cylinder axis, we may expect that in the context of magnetic fusion with machines with large aspect ratios the presence of zonal flows along the toroidal direction is important to increase confinement. Going back to our simple model, since the safety factor $q(r)$ can be directly associated with the function $F(r)$ at the origin of the unstable fixed points, and $q(r)$ is a crucial parameter for the operation of magnetized fusion machine, let us discuss more how the constraints discussed previously translate on the q -profile. For instance let us consider a situation with a non-monotonous profile such that $q(r)$ has a minimum q_0 at $r = \alpha$ and the spatial scale is characterized with λ . Then locally $q(r)$ can be expressed as

$$q(r) = q_0 [1 + \lambda^2(r - \alpha)^2], \quad r \sim \alpha. \quad (13)$$

Recalling Eq. (1), the function F is scaled as $q_0^{-1}\lambda^{-1}$, and $v_z^2/2 = (p_z + F)^2/2 \sim q_0^{-2}\lambda^{-2}$, so that this provides a typical energy level of the particles located near a separatrix. It should be noted that the width of the well of $v_z^2/2$ scales as λ^{-1} (see Fig. 1). For a fixed value of q_0 , a large value of λ creates unstable fixed points with relevant energy levels for the particle whose angular momentum is $p_\theta \sim B_0\alpha^2/2$. As λ gets to be larger, the number of the particles with un-

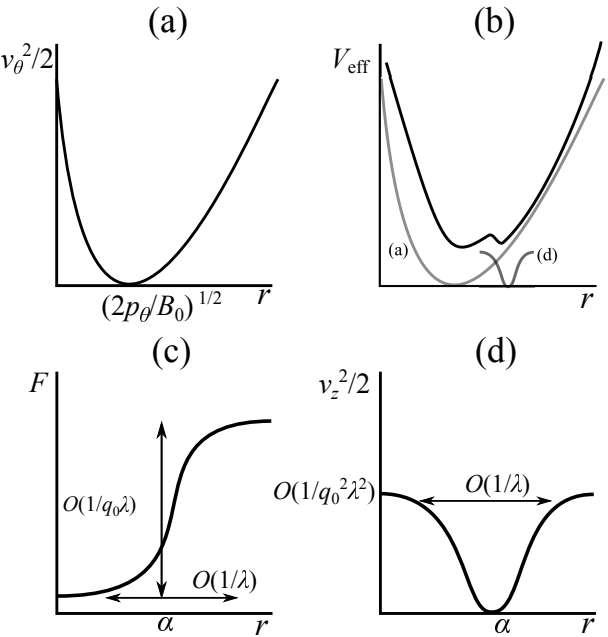


FIG. 1. Schematic picture showing how the saddle point appears around the bottom of safety factors. A Panel (a) represents a part of $v_\theta^2/2 = (p_\theta/r - B_0 r/2)^2/2$, (b) V_{eff} , (c) $F(r)$, and (d) $v_z^2/2 = (p_z + F(r))^2/2$. In the panel (d), we consider that there exists an r such that $p_z + F(r) = 0$. The parameters q_0 , λ , and α are associated with Eq. (13).

stable fixed point increase. This is because, roughly speaking, the energy levels of unstable points get to be lower, and the one-particle density (5) is proportional to $e^{-\beta H_{\text{eff}}}$. As a consequence of these considerations we illustrate on Fig. 2 how to adjust a given q -profile in order to create unstable fixed points whose location is $r \sim \alpha$. One can set up unstable fixed point around $r \sim \alpha$ by modifying the q -profile so that it has concavity around $r = \alpha$.

We then have a form of density profile (10) and a condition for q -profile exhibiting unstable fixed points. We next consider where the unstable points appear, and we shall exhibit that the emergence of unstable fixed points induces the presence of a local steep profile in their vicinity, *i.e.* their radial positions are inducing the existence of locally strong density gradients. For this purpose we simply consider the q -profile given by Eq. (13) with parameters $q_0 = 0.12$, $\lambda = 55$, and $\alpha = \sqrt{0.18} \simeq 0.4243$, in Figs. 3. When including perturbations, we point out that the adiabatic chaos due to separatrix crossing in this magnetic field has been discussed in Ref. [11]. The results are displayed in Fig. 3, where two density profiles (10) obtained for two q -profiles with and without unstable fixed points are shown. The parameter α is changed so that they have same density in the center of cylinder. We note α can be changed keeping the thermodynamical temperature β^{-1} and changing the average of angle velocity v_θ . We find the steep region which corresponds to the local steep density gradient around $r = \alpha$ on which $q(r)$ satisfies $q'(r) = 0$ for the q -profile with unstable points. Going further on, reasoning directly with a q -profile

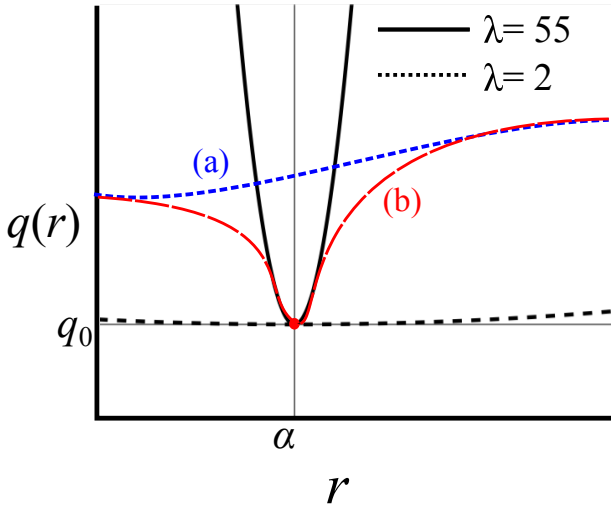


FIG. 2. Schematic picture exhibiting how to create unstable fixed point by modifying q -profile. The solid curve represents the given q -profile. Dotted and bold curves are the graph of $q_0(1+\lambda^2(r-\alpha)^2)$ for $q_0 = 0.12$, $\alpha = \sqrt{0.18}$ and $\lambda = 2, 55$ respectively. The $q(r)$ with $\lambda = 55$ induces the unstable fixed points, so does not one with $\lambda = 2$. (a) and (b) correspond respectively to the q -profiles without and with unstable fixed points.

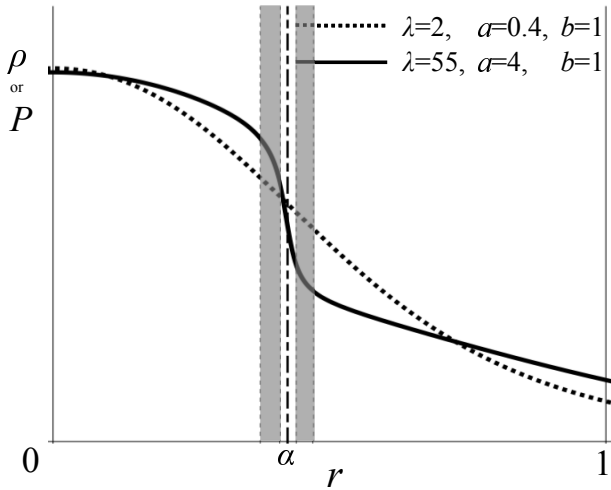


FIG. 3. (Color online) The solid and dotted curves express the density profiles with q -profiles with unstable points (shaded region) and without unstable points respectively. The parameters in a local q -profile [Eq. (13)] are determined as $q_0 = 0.12$, and $\alpha = \sqrt{0.18} \approx 0.4243$, and $\lambda = 55$ for the solid curve and $\lambda = 2$ for the dotted one. In both profiles, γ_z and β are same, but γ_θ is different.

may lead to some physical problems. For a given magnetic configuration inspired from a tokamak, the toroidal component of the magnetic field is generated by the current within the plasma. In the large aspect ratio (cylindrical) limit, this readily gives a r dependence of the current

$$j(r) = \frac{1}{r} \frac{\partial}{\partial r} \left(r \frac{\partial F}{\partial r} \right). \quad (14)$$

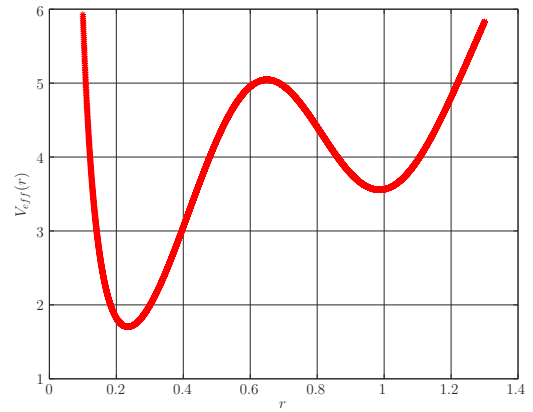


FIG. 4. (Color online) Effective potential for $F(r) = F_0 J_2(\lambda r)$. An Unstable point appears as expected around $r_0 = 0.6$. Here we choose the parameters as $F_0 = 1$, $p_\theta = 0.5$, $p_z = 1$, $B_0 = 4$.

When looking at the current profile given by the q -profile giving rise to Fig. 3, we end up with two different region one, with a negative current for r sufficiently large, and one with a positive one for small r . This is likely to be physically not realistic. Eventhough it may have appeared as possible, the actual stability of these configuration is doubtful, see for instance [29–31]. In order to generate a profile that could be more physically relevant, we may have again a look at Eq. (10). We can notice that a “steep” variation of the function $F(r)$ will likely trigger a steepness in the density profile. Taking into account Eq. (14), we can look for profiles that can achieve this variation while keeping a positive current. Given the form of Eq. (14), it appears as simpler to look for just one Bessel function of the first kind $F = F_0 J_\nu(\lambda r)$ and to create only one separatrix, we consider the case when no plasma current is present, then the minimum of the effective potential (2) is located at r_0 such that $p_\theta = B_0 r_0^2/2$. Given the expression (14), and our choice of F , expecting some current in $r = 0$, implies that $\nu = 2$, we adjust λ to keep a positive current up to $R = 1$, which leads to $\lambda = 1/r_1$, with r_1 being the first zero of $J_2(r)$. The shape of J_2 , leads to expect a maximum near $r = 1/2$ for F , so we can expect that by tuning the parameters a and b , we will capture many r_0 ’s (for the different p_θ ’s), giving rise to regions in phase space with separatrices that have non-negligible statistical weights. An illustration of possible obtained profiles are depicted in Fig. (5).

Before concluding this letter we would like to make some remarks on the observed profiles which indicate the presence of what we may call an ITB although the underlying physical mechanisms are quite different. We would like to stress out the similarities our observations and the magnetic ITBs discussed for instance in [19]. One of the main difference is that if the plateau of $q(r)$ appears the transport barrier emerges even if the value of q is far from rational number m/n with small integers m and n , in that sense the creation of the barrier with the q -profile (13) is not correlated to the existence of a resonant surface, on the other hand for

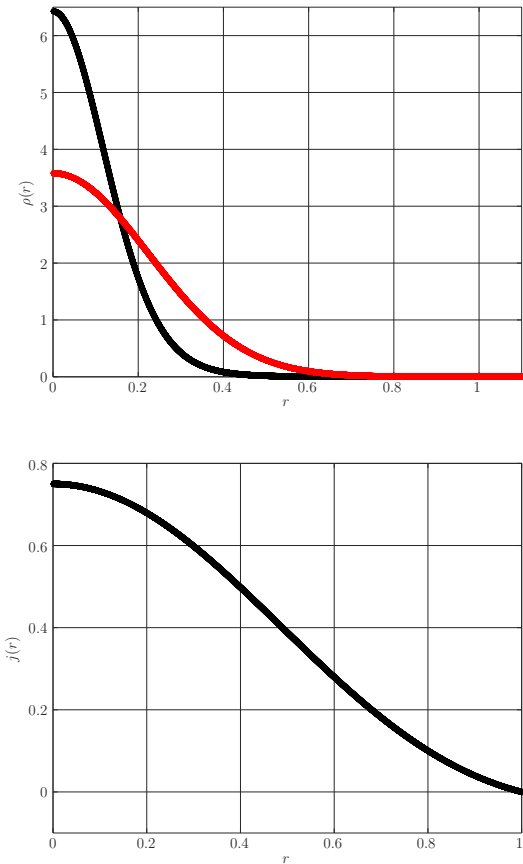


FIG. 5. (Color online) Top: The gray(red) and black curves express the density profiles with only one unstable point. Bottom: same current profile for both configurations. The parameters are $F_0 = 1$, $a = b = 10$ for the gray(red) curve $F_0 = 1$, $a = 10$, $b = 0$ for the black.

the considered example, we can notice that the location of the magnetic ITB coincides with the place on which the local density gradient exists.

Another study between the particle's motion and the existence of an ITB using a pure field line approach and the existence of a stable magnetic tori has been performed from the view point of the difference between the magnetic winding number $q(r)$ and the effective one $q_{\text{eff}}(r)$ for the guiding venter orbit of the energetic particles [25]. In a recent study [26], it is shown that the resonance shift due to the grad B drift and its disappearance due to the curvature drift effect can create an invariant tori in the particle dynamics while there are none for magnetic field lines, and this is confirmed both analytically and numerically with the full particle orbits around the resonance points. It should be remarked that the guiding center theory is useless to clarify it unlike Ref. [26].

The above consideration provides de facto another difference between the magnetic ITB and the effective ITB induced by the separatrices. Moreover, we can stress out that the magnetic ITB is present in both situations described in Fig. 3, while the steep profile occurs only when the hyperbolic points are present. When considering the degenerate q -profile we also note that the two unstable fixed points appear around the magnetic ITB and when the parameter λ in Eq. (13) gets to be large, the steep region of $\rho(r)$ gets to be strong as the influence of the separatrix grows because the gap of $F(r)$ between $r < \alpha$ and $r > \alpha$ becomes smaller (see Fig. 1).

To conclude, we have shown in this letter that steep equilibrium density profiles can emerge due to the presence of a separatrix in the passive particle orbits, this phenomenon is not related to the existence of a local resonant surface and the observed phenomenon is reminiscent of the presence of an ITB although the physical mechanisms inducing it are a priori quite different in interpretation. We also discussed how the q -profile can be tuned in order to generate such barriers.

We finally remark on what happens if we consider a toroidal configuration. Let us imagine our cylindrical system is an infinite toroidal radius limit of the toroidal system as Ref. [12]. The finite toroidal radius effect breaks the integrability and it thus can induces adiabatic chaos. It has been known for a while that the presence of chaos affects sometimes the density profile locally. For instance, the averaging effect in plasmas from the global chaos induced by the resonance overlapping [27] has been found and it modifies the density profile [28]. Even though we are directly tackling the passive particle motions of ions and thus a different type of localized chaos in this letter, similar things can be expected. In the present case the unstable fixed points are located around the place in which the steepness of density (10) and the local pressure gradient exist as shown in Fig. 3. Therefore the flattening effect makes them steeper locally. As a result we can expect that this steepening effect observed in the cylindrical configuration can be robust at least as long as strongly chaotic motion remains localized near each hyperbolic point.

ACKNOWLEDGMENTS

S. O. and X. L. thank G. Dif-Pradalier for useful and encouraging discussions. X. L. thanks E. Laribi for careful reading of the manuscript. This work has been carried out within the framework of the French Research Federation for Magnetic Fusion Studies. The project leading to this publication has received funding from Excellence Initiative of Aix-Marseille University - AMIDEX, a French “Investissements d'Avenir” programme.

[1] R. C. Wolf, Plasma Phys. Control. Fusion **45** (2003) R1.

[2] J. W. Connor, T. Fukuda, X. Garbet, C. Gormezano, V. Mukhovatov, M. Wakatani, ITB Database Group, and ITPA Topical

Group on Transport and Internal Barrier Physics, Nucl. Fusion **44** (2004) R1.

[3] H. Alfvén, Ark. Mat. Astron. Fys. **27A** (1940) 1; *Cosmological electrodynamics*, (Oxford university press, London, 1950).

[4] T. G. Northrop, Ann. Phys. **15** (1961) 79.

[5] R. G. Littlejohn, Phys. Fluids **24** (1981) 1730.

[6] A. H. Boozer, Rev. Mod. Phys. **76** (2004) 1071.

[7] J. R. Cary and A. J. Brizard, Rev. Mod. Phys. **81** (2009) 693.

[8] A. J. Brizard and T. S. Hahm, Rev. Mod. Phys., **79** (2007) 421.

[9] J. D. Jackson, *Classical Electrodynamics, 3rd ed.* (Wiley, USA, 1998).

[10] D. Pfefferl, J. P. Graves, and W. A. Cooper, Plasma Phys. Controlled Fusion **57** (2015) 054017.

[11] S. Ogawa, B. Cambon, X. Leoncini, M. Vittot, D. del-Castillo-Negrete, G. Dif-Pradalier, and X. Garbet, Phys. Plasmas **23** (2016) 072506.

[12] B. Cambon, X. Leoncini, M. Vittot, R. Dumont, and X. Garbet, Chaos **24** (2014) 033101.

[13] A. I. Neishtadt, Sov. J. Plasma Phys. **12**, 568 (1986).

[14] A. I. Neishtadt, Prikl. Matem. Mekhan. USSR **51** (1987) 586.

[15] J. L. Tennyson, J. R. Cary, and D. F. Escande, Phys. Rev. Lett. **56** (1986) 2117.

[16] J. R. Cary, D. F. Escande, and J. L. Tennyson, Phys. Rev. A **34** (1986) 4256.

[17] X. Leoncini, A. Neishtadt, and A. Vasiliev, Phys. Rev. E **79** (2009) 026213.

[18] R. Balescu, Phys. Rev. E **58** (1998) 3781.

[19] D. Constantinescu and M.-C. Firpo, Nucl. Fusion **52** (2012) 054006.

[20] A. A. Vlasov, Zh. Eksp. Ther. Fiz. **8** (1938) 291; Sov. Phys. Uspekhi **93** (1968).

[21] L. P. Pitaevskii and E.M. Lifshitz, *Physical Kinetics* (Butterworth-Heinemann, Oxford, 1981)

[22] T. M. Rocha Filho, A. Figueiredo, and M A. Amato, Phys. Rev. Lett. **95** (2005) 190601.

[23] X. Leoncini, T. L. Van den Berg and D. Fanelli, EPL **86** (2009) 20002.

[24] D. Zubarev, V. Morozov, and G. Ruppek, *Statistical Mechanics of Nonequilibrium Processes, Volume 1: Basic concepts, kinetic theory* (Academic Verlag, Berlin, 1996).

[25] G. Fiksel, B. Hudson, D. J. Den Hartog, R. M. Magee, R. O'Connell, and S. C. Prager, Phys. Rev. Lett. **95** (2005) 125001.

[26] S. Ogawa, X. Leoncini, G. Dif-Pradalier, and X. Garbet, Phys. Plasmas **23** (2016) 122510.

[27] B. V. Chirikov, Phys. Rep. **52** (1979) 263.

[28] R.B. White, Commun. Nonlinear Sci. Numer. Simulat. **17** (2012) 2200; Plasma Phys. Control. Fusion **53** (2011) 085018.

[29] G. T. A. Huysmans, T. C. Hender, N. C. Hawkes, and X. Litaudon, Phys. Rev. Lett. **87** (2001) 245002.

[30] G. W. Hammett, S. C. Jardin, and B. C. Stratton, Phys. Plasmas **10** (2003) 4048.

[31] Yu. I. Pozdnyakov, Plasmas **12** (2005) 084503.